**RESEARCH ARTICLE**

# Terpene Derivatives: A Comprehensive Computational Insights in Drug-likeness and ADMT Properties, and DFT Study

**Goncagül Serdaroğlu¹\*** 🆔

¹Sivas Cumhuriyet University, Faculty of Education, Math. and Sci. Edu., 58140, Sivas, Turkey

**Abstract**: In this study, the terpene-like compounds were investigated to explore the possible reactivity tendency using DFT/B3LYP/6-311G** level and evaluation of absorption, distribution, and metabolism characteristics. The lipophilicity indexes of terpenes revealed that the T1 and T2 molecules were more lipophilic than the other molecules, whereas the T5 and T6 molecules were less lipophilic. The water solubility scores obtained from ALI and ESOL approaches indicated that T5 and T6 functionalized with the -C=O group's most soluble compounds, while T2 was the least soluble among the compounds. Regarding absorption, the T5 molecule was determined to be a promising structure among the compounds. Also, all compounds' VD (L/kg) values were determined in the optimal range of 0.04-20 L/kg. The terpenes T1-T3 would exhibit a BBB Penetration at a medium level, while they would not be suitable structures for PPB %. The terpenes T4-T6 could be quite promising in distribution except for BBB Penetration. T6 structure was determined to be more suitable in terms of metabolism than the other terpenes. NBO analyses revealed that cieplak ($\sigma \rightarrow \sigma^*$) interactions for T1-T4 would lower the stabilization energy, predicted at 7.04 kcal/mol. In contrast, the resonance ($\pi \rightarrow \pi^*$) interaction for T5 was predicted with the energy of 20.26 kcal/mol, which was the highest contributed interaction to $E^{(2)}$. FMO analyses indicated that T5 (0.204 au) could prefer electron donation more than terpenes, while T4 (0.108 au) would prefer electron donation less. MEP plots implied that the surround of the oxygen atom for T3-T6 molecules would be the electron-rich region for the electrophiles, whereas the around of the double bonds of T1 and T2 would be possible sites for the electrophiles. According to the NPA approach, the atomic charge of the O1 atom of terpenes T4-T6 was predicted at -0.76279, -0.55670, and -0.55395, whereas the O28 atom' charge was found to be at -0.77131, remarkable. The findings from this study are anticipated to provide invaluable insights into the relationship between electronic structure, ADM properties, and toxicity. This could potentially guide the future discovery, development, and refinement of terpene-based therapeutics.

## 1. INTRODUCTION

Terpenes and terpenoids are a broad and diverse class of naturally occurring organic compounds produced by a wide variety of plants, fungi, and bacteria (1-3). Due to their strong odors, they play a critical role in plant biology, especially in defense mechanisms against herbivores and in plant-to-plant and plant-to-environment interactions (4). Furthermore, they have been found to possess a broad range of biological activities (5), including anti-inflammatory (6), antiviral (7), antibacterial (8), and anticancer (9,10). Thus, the application of terpenes is extensive and extends to fields like pharmaceuticals, food additives (11,12), cosmetics (13,14), and even biofuels (15,16). In this regard, Pahima et al. (16) presented a model that combined theoretical and statistical approaches to calculate the thermodynamic properties of terpenes, a promising biofuel. It accurately computes key properties using advanced computational methods, offering a cost-effective strategy for identifying potential petroleum substitutes without expensive experiments. In this regard, coumarin and its nitrile-modified derivative have been investigated by using electrochemical tools and DFT computations to explore the possible

inhibition potency on mild steel surfaces (17). Furthermore, the key interactions between purine metabolism products and DNA have also been investigated by using electrochemical techniques and DFT computational tools (18). Recently, the highly selective fluorescent ligand 3-(1H-benzimidazol-2-yl)quinolin-2(1H)-one monohydrate has been designed and explored in terms of sequential sensing of Cu(II) and HS- ions in the solution (19). In recent work, Maspero and co-workers have reported a novel strategy to explore the possible enhancement of fluorescence characteristics of the biocompatible difluoro boron-functionalized biindolediketonates: they have also performed TD-B3LYP-D3 computations to characterize the $s_0 \rightarrow s_1$ transition (20). Carvomenthene, Limonene, 4-Terpinenol, α-terpineol, and Carvone are also key members of the terpene family, characterized by unique structures, all of which are constructed from isoprene units and reflecting the inherent structural design of terpenes (21). Namely, limonene, a monocyclic monoterpene, is one of the most common terpenes. It is known for its citrusy aroma and is a principal constituent in citrus peel oils (22). 4-Terpinenol, α-terpineol, and carvomenthene, like limonene, are monoterpenes with distinctive structural arrangements and biochemical characteristics. Conversely, carvone is a monoterpene ketone, presenting as two mirror-image forms or enantiomers, each with a distinct minty or caraway aroma (23).

To understand the biological activity and physicochemical properties of terpenes (Scheme 1), it's important to delve into their structural composition and molecular behavior. In this regard, computational chemistry, specifically Density Functional Theory (DFT), has shown promising results. DFT has been extensively used to study terpenes' molecular geometries, electronic structures, and reaction mechanisms (24-26). Such theoretical studies aid in revealing the fundamental structure-activity relationships, paving the way for the development of new applications and fine-tuning existing uses of these fascinating molecules. In a recent work on carvone, Yankova et al. focused on the electronic properties and chemical activity of carvone by using a B3LYP level with a 6-311++G(2d,2p) basis set; they performed the NBO, FMO, and MEP studies as well as the Hirshfeld surface (27). Also, Mekkaoui and co-workers (28) synthesized the optically active limonaketone with a 92% yield, a high-value monoterpene, from natural and inexpensive limonene and explored the chemoselectivity in the Zinc-deoxygenation reaction and its corresponding mechanistic pathway using density functional theory (DFT) calculations at the M06–2X/6–311G(d,p) (LANL2DZ for Zinc) level.
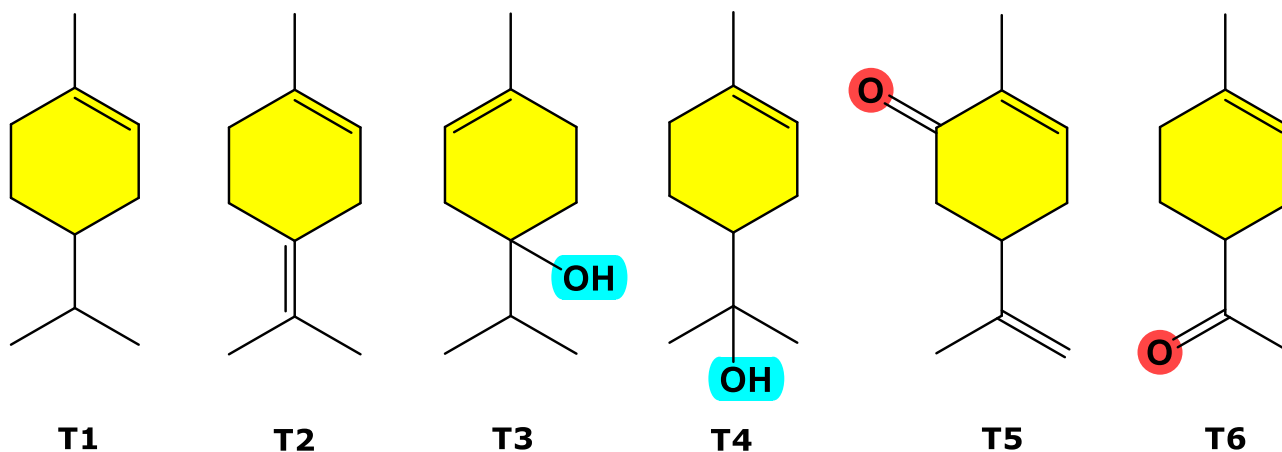


**Scheme 1:** The chemical structures of terpenes: The abbreviations and common names are as follows
***T1***: 4-isopropyl-1-methylcyclohex-1-ene (Carvomenthene)
***T2***: 1-methyl-4-(propan-2-ylidene)cyclohex-1-ene ( Limonene)
***T3***: 1-isopropyl-4-methylcyclohex-3-en-1-ol (4-Terpinenol)
***T4***: 2-(4-methylcyclohex-3-en-1-yl)propan-2-ol (α-terpineol)
***T5***: 2-methyl-5-(prop-1-en-2-yl)cyclohex-2-en-1-one (Carvone)
***T6***: 1-(4-methylcyclohex-3-en-1-yl)ethan-1-one (Limonaketone)

Terpenes such as carvomenthene (T1), limonene (T2), 4-terpineol (T3), α-terpineol (T4), carvone (T5), and limonaketone (T6) are prime examples of the diverse structural composition and inherent design of terpenes. Understanding their unique structures and molecular behavior is key to revealing their biological activity and physicochemical properties. In this perspective, the DFT computational tools have been particularly effective in studying the molecular geometries, electronic structures, and reaction mechanisms of terpenes and related compounds. Also, the application of computational methods like DFT enables researchers to delve deeper into the complex world of these molecules, promoting their potential in various applications and helping address global challenges such as the need for renewable energy sources. The main idea of this paper is to present a comprehensive overview of the compounds T1-T6 structurally related to the terpenes, covering their structures, biological importance, and possible harmful effects in terms of both medicinal and environmental. By the advantages of the DFT computations, this work will be hoped to support the smart molecule design,

introducing the electronic and related properties that are important in developing or modifying the molecular systems.

## 2. COMPUTATIONAL METHODS

### 2. 1. DFT Study
All DFT computations at the B3LYP (29,30) /6-311G** (31,32) level of theory maintaining default (33,34) settings were performed using the G09W (35), which were also utilized by GaussView 6.0.16 (36) for demonstrating the optimized structures and FMO plots. The water phase simulations were conducted using the PCM "Polarized Continuum Model" (37,38).

It is well-established that the evaluation of thermodynamic quantities is guided by the principles of quantum statistics (39,40). Namely, the total partition function 'Q' is instrumental in the determination of thermodynamic properties via specific equations outlined herein. In systems typified as asymmetric tops, the vibrational degree of freedom amounts to 3N-6, attributable to the molecular systems having three translational freedom degrees and three rotation freedom degrees along separate axes. Therefore, it is imperative to understand that variations in the quantities of thermodynamic properties across all molecular systems originate remarkably from vibrational movements since the contributions from translational and rotational movements remain consistent. The formulation of the vibrational partition function, as presented below, plays a vital role in contributing to thermodynamic properties and, by extension, is crucial in the evaluation of chemical properties (39-42).

$$Q = Q_{trans.} \; x \; Q_{rot.} \; x \; Q_{vib.} \; Q_{elec.}$$
$$Q_{vib.} = \prod_{j=1}^{3N-6} \frac{e^{-\Theta_{v,j}/2T}}{\left(1 - e^{-\frac{\Theta_{vj}}{T}}\right)}$$

Here, $E_{vib.}$ "vibrational thermal energy", $S_{vib.}$ "vibrational entropy", and $Cv_{vib.}$ "vibrational heat capacity" are calculated by the following equations (39-41).

$$E_{vib.} = Nk \sum_{j=1}^{3N-6} \left( \frac{\Theta_{v,j}}{2} + \frac{\Theta_{vj} \; e^{-\Theta_{v,j}/T}}{\left(1 - e^{-\frac{\Theta_{v,j}}{T}}\right)} \right)$$

$$S_{vib} = Nk \sum_{j=1}^{3N-6} \left[ \frac{\Theta_{v,j}/T}{\left(e^{\Theta_{v,j}/T} - 1\right)} - ln\left(1 - e^{-\Theta_{v,j}/T}\right) \right]$$

$$Cv_{vib.} = Nk \sum_{j=1}^{3N-6} \left[ \left(\frac{\Theta_{vj}}{T}\right)^2 \frac{e^{\Theta_{vj}/T}}{\left(e^{\Theta_{v,j}/T} - 1\right)^2} \right]$$

The terms disclosed as $\Theta_{vj} = \frac{h v_j}{k}$ "the vibrational temperature", h→ "Planck constant", k→ "Boltzmann constant", and $v_j$→" $j^{th}$ fundamental frequency".

Koopmans' theorem delineates the parameters of 'ionization energy' (I) and 'electron affinity' (A) (43), contingent on the energies of the frontier molecular orbitals. After the derivation of I and A values, the computation of global reactivity indices

can be achieved through the employment of the ensuing equations.

$I= -E_{HOMO}$
$A= -E_{LUMO}$
$\chi = -(\frac{I+A}{2})$
$\eta = \frac{I-A}{2}$
$\omega = \frac{\mu^2}{2\eta}$
$$\Delta N_{max} = \frac{I+A}{2(I-A)}$$
$\omega^+ \approx (I + 3A)^2/(16(I-A))$
$\omega^- \approx (3I + A)^2/(16(I-A))$
$$\Delta \varepsilon_{back-donation} = -\frac{\eta}{4}$$

The symbols denoted that $\chi$ → "electronic chemical potential" $\eta$ → "global hardness", $\omega$ → "electrophilicity", $\Delta N_{max}$ → "the maximum charge transfer capability index" (44-49), $\omega$- "the electron donating power" and $\omega$+ "the electron accepting power" (50), and $\Delta E_{back-donat.}$ "back-donation energy" (51).

The "second-order-perturbation" energy analyses and NPA "Natural population analysis" of terpenes T1-T6 were performed using the NBO code (52) implemented in the G09W. Accordingly, the lowering stabilization energy depending on the $q_i$→ "the donor orbital occupancy", $\varepsilon_i$ and $\varepsilon_j$→ "donor and acceptor orbital energies (diagonal elements)", $F_{ij}$→ "the off-diagonal NBO Fock matrix element" is defined as follows (53-56):

$$E^{(2)} = \Delta E_{ij} = qi \frac{(Fij)^2}{(\varepsilon j - \varepsilon i)}$$

In addition to the NPA approach, MPA "Mulliken Population Analysis" (57) is used to evaluate the partial charges of terpenes.

### 2. 2. Lipophilicity and water solubility
The estimation of lipophilicity indices was comprehensively undertaken employing a suite of five distinct methodologies, namely, ILOGP (58), XLOGP3 (59), WLOGP (60), MLOGP (61), and SILICOS-IT (62). The execution of these methodologies was facilitated via the SwissADME tool (63). It is widely recognized in scientific discourse that the parameter for lipophilicity, denoted as Log P, is inherently based on the ratio of the concentration of a specific neutral molecular system in an octanol medium (Co) to its concentration in a water medium (Cw). This principle is encapsulated in the following mathematical formulation.

$$Log \; P_{o/w} = Log \; \frac{C_o}{C_w}$$

The calculation of water solubility, represented as Log S, was carried out using distinct methodologies as delineated by Delaney et al. (64) and Ali et al. (55). Here, the 'Estimated SOLubility' (ESOL) method defined by Delaney et al. (44) is employed, which derives its calculation based on specific molecular characteristics. These characteristics include 'Molecular Weight' (MWT), 'Rotatable Bonds

(RB), and 'Aromatic Proportion' (AP). The following equations delineate this approach.

Log *Sw*= 0.16-0.63 clogP - 0.0062 MWT + 0.066 RB - 0.74 AP (ESOL)

Furthermore, a robust benchmark study by Ali et al. (65) demonstrated a notable correlation between water solubility and specific phenolic parameters, such as the number of aromatic hydroxyls (-OH) groups. Additional factors, including the melting point and Topological Polar Surface Area (TPSA), were also found to impact water solubility significantly, as explained in the following equations.

logS= -1.0239 logP- 0.0148 TPSA- 0.0058 (m.p. (C)- 25)+ 0.3295 aroOHdel+ 0.5337 (ALI)

## 2. 3. Absorption, Distribution, Metabolism, and Toxicity
Evaluation of the drug-like properties of **T1-T6** was comprehensively undertaken, guided by a selection of established rules and parameters as defined by Lipinski (61), Ghose (66), Veber (67), Egan (68), and Muegge (69). In addition, the Abbott bioavailability score (70) was employed as an instrumental tool in assessing the potential bioavailability of **T1-T6** with the aid of the SwissADME platform (63). To gain a holistic understanding of the dataset's pharmacokinetic properties, its absorption, distribution, metabolism, and potential toxicity characteristics were delineated utilizing the capabilities of ADMETLab 2.0 (71).

## 3. RESULT AND DISCUSSION

### 3. 1. Calculated Thermochemical and Physical Properties
Within the complex domain of molecular characterization, thermochemical and physical parameters serve as fundamental constituents. Thermochemical components, incorporating parameters such as heat capacity, enthalpy, and entropy, elucidate the molecule's stability and reactivity and delineate potential energy profiles. Concurrently, physical indices, including molecular weight, geometric configuration, and polarity, provide a detailed representation of the molecule's intrinsic physical comportment, influencing attributes such as solubility and reactivity (72-75). Thereby, they facilitate a holistic comprehension of

molecular properties and, then, the conceptualization and advancement of novel molecular structures across diverse scientific and industrial spheres. In this regard, the calculated thermodynamic quantities of the optimized molecules T1-T6 (Figure 1) and physical constants are presented in Table 1.

In the gas phase, the DM (D) and α (au) values of T1-T6 were found to be in the orders of T2 (0.205)< T1 (0.216)< T4 (1.562)< T3 (1.659)< T6 (2.729)< T5 (2.981) and T6 (98.979)< T5 (111.613)< T1 (112.485)< T2 (114.182)< T3 (114.749)< T4 (115.705), respectively, the water phase revealed the same orders for both properties. ΔGsol. (kJ/mol) order was determined as T5 (18.879)> T6 (17.78)> T4 (14.26)> T3 (11.94)> T2 (5.97)> T1 (4.64), which indicated that T5 and T6 would gain more stability in water than the others, probably due to the presence of the -C=O (ketone) group. $\Delta E_{sol.}$ and $\Delta H_{sol.}$ (kJ/mol) values of T1-T6 were found to be as T5 (18.92)> T6 (18.13)> T4 (14.25)> T3 (11.67)> T2 (6.14)> T1 (4.62) and T5 (18.97)> T6 (18.19)> T4 (14.21)> T3 (11.52)> T2 (6.16)> T1 (4.59), respectively. The main participation of both entropy and heat capacity was sourced from the vibrational freedom degrees, as expected. The $\Delta E_{thermal}$ (kcal/mol) for T1 was determined to be 168.523 kcal/mol by the vibrational contribution of 166.746 kcal/mol, which is remarkable. Similarly, the Cv quantity of T6 was found to be 39.643 cal/molK by the vibrational contribution of 33.681cal/molK. From Table 1, the $\Delta E_{thermal}$ (kcal/mol) and Cv (cal/molK) of the T1-T6 were estimated as the orders of T3 (171.915)> T4 (171.789)> T1 (168.523)> T2 (153.413)> T5 (142.2367)> T6 (138.568) and T4 (48.251)> T3 (48.173)> T1 (43.428)> T2 (42.390)> T5 (43.277)> T6 (39.643), respectively. Also, the S (cal/molK) values of the compounds were calculated as T4 (106.316)> T3 (105.776)> T5 (105.187)> T2 (103.073)> T1 (102.074)> T6 (100.069), and vibrational freedom degrees of all compounds constituted one-third of entropy. By analyzing and comparing these parameters, the obtained results not only provide a deeper understanding of the physical and chemical properties of these compounds but also present valuable insights into their behavior under diverse environmental conditions. Thus, they can effectively guide the design and development of new materials that possess desired and tailored properties for a wide range of applications.

**Table 1:** The calculated physiochemical values.

|  |  | T1 | T2 | T3 | T4 | T5 | T6 |
|---|---|---|---|---|---|---|---|
| **Gas** | DM (debye) | 0.216 | 0.205 | 1.659 | 1.562 | 2.981 | 2.729 |
| | α (au) | 112.485 | 114.182 | 114.749 | 115.705 | 111.613 | 98.979 |
| | ΔE (au) | -391.753938 | -390.549241 | -466.990430 | -466.990042 | -464.603006 | -426.509962 |
| | ΔH (au) | -391.741759 | -390.537018 | -466.977195 | -466.976767 | -464.590580 | -426.498496 |
| | ΔG (au) | -391.790258 | -390.585991 | -467.027453 | -467.027281 | -464.640557 | -426.546042 |
| | ΔE$_{thermal}$ (kcal/mol) | 168.523 | 153.413 | 171.915 | 171.789 | 142.236 | 138.568 |
| | ΔE$_{vib.}$ (kcal/mol) | 166.746 | 151.635 | 170.138 | 170.012 | 140.459 | 136.790 |
| | Cv (cal/molK) | 43.428 | 42.390 | 48.173 | 48.251 | 43.277 | 39.643 |
| | Cv$_{vib.}$ (cal/molK) | 37.466 | 36.428 | 42.211 | 42.290 | 37.315 | 33.681 |
| | S (cal/molK) | 102.074 | 103.073 | 105.776 | 106.316 | 105.187 | 100.069 |
| | S$_{vib}$ (cal/molK) | 31.473 | 32.600 | 34.580 | 34.946 | 33.917 | 29.807 |
| **Water** | DM (debye) | 0.338 | 0.323 | 2.142 | 2.098 | 4.094 | 3.825 |
| | α (au) | 148.303 | 150.294 | 150.970 | 151.762 | 147.378 | 129.850 |
| | ΔE (au) | -391.755697 | -390.551580 | -466.994876 | -466.995468 | -464.610213 | -426.516866 |
| | ΔH (au) | -391.743508 | -390.539364 | -466.981582 | -466.982180 | -464.597806 | -426.505424 |
| | ΔG (au) | -391.792027 | -390.588264 | -467.032000 | -467.032712 | -464.647746 | -426.552815 |
| | ΔE$_{thermal}$ (kcal/mol) | 168.193 | 153.144 | 171.581 | 171.494 | 142.066 | 138.412 |
| | ΔE$_{vib.}$ (kcal/mol) | 166.415 | 151.366 | 169.804 | 169.717 | 140.288 | 136.635 |
| | Cv (cal/molK) | 43.528 | 42.470 | 48.342 | 48.355 | 43.287 | 39.661 |
| | Cv$_{vib.}$ (cal/molK) | 37.567 | 36.508 | 42.380 | 42.394 | 37.326 | 33.699 |
| | S (cal/molK) | 102.117 | 102.918 | 106.115 | 106.353 | 105.109 | 99.742 |
| | S$_{vib}$ (cal/molK) | 31.515 | 32.443 | 34.914 | 34.978 | 33.839 | 29.485 |

| *Solvation energies* |  |  |  |  |  |  |
|---|---|---|---|---|---|---|
| ΔE$_{sol.}$ (kJ/mol) | 4.62 | 6.14 | 11.67 | 14.25 | 18.92 | 18.13 |
| ΔH$_{sol.}$ (kJ/mol) | 4.59 | 6.16 | 11.52 | 14.21 | 18.97 | 18.19 |
| ΔG$_{sol.}$ (kJ/mol) | 4.64 | 5.97 | 11.94 | 14.26 | 18.87 | 17.78 |

### 3.2. Lipophilicity and water solubility

In the field of pharmaceutical research and development, two crucial factors that come into play are the hydrophobicity (fat-solubility) and hydrophilicity (water-solubility) of organic compounds (76). Hydrophobicity significantly impacts the processes of drug absorption, distribution, metabolism, and excretion (77), and highly hydrophobic drugs carry the risk of accumulating in the body's adipose tissues and causing toxicity (78). Conversely, hydrophilicity plays a pivotal role in drug formulation, delivery, and bioavailability, posing challenges when a drug exhibits excessively high or low water solubility. Both hydrophobicity and hydrophilicity contribute to drug-drug interactions and chemical stability, ultimately influencing drug effectiveness, safety, and overall suitability (79). In this respect, the calculated lipophilic and water solubility characteristics and physicochemical values of T1-T6 are given in Table 2.

Log Po/w (iLOGP) indices were determined in the following order T1 (2.74)> T2 ( 2.71)> T3 (2.51)> T5 (2.27)> T4 (2.09)> T6 (2.03), while the lipophilicity index depending on (XLOGP3) approach was estimated as T1 (3.42)> T2 (4.47)> T4 (3.39)> T3 (3.26)> T5 (2.71)> T6 (1.34). On the other hand, the WLOGP approach to determine the lipophilicity revealed the following order: T2 (3.45)> T1 (3.39)> T3 (2.50)≥ T4 (2.50)> T5 (2.49)> T6 (2.32), whereas the Log Po/w based on MLOGP. the approach was predicted as T1 (4.29)> T2 (3.27)> T3 (2.30)≥ T4 (2.30)> T5 (2.10)> T6 (1.89). The mean of the lipophilicity indices changed in the following order: T2 (3.40)> T1 (3.36)> T3 (2.60)> T4 (2.49)> T5 (2.44)> T6 (1.98). Although the approaches used to calculate the lipophilicity index had different rankings, it could be said that the lipophilicity of the T1 and T2 molecules was higher than the other molecules.
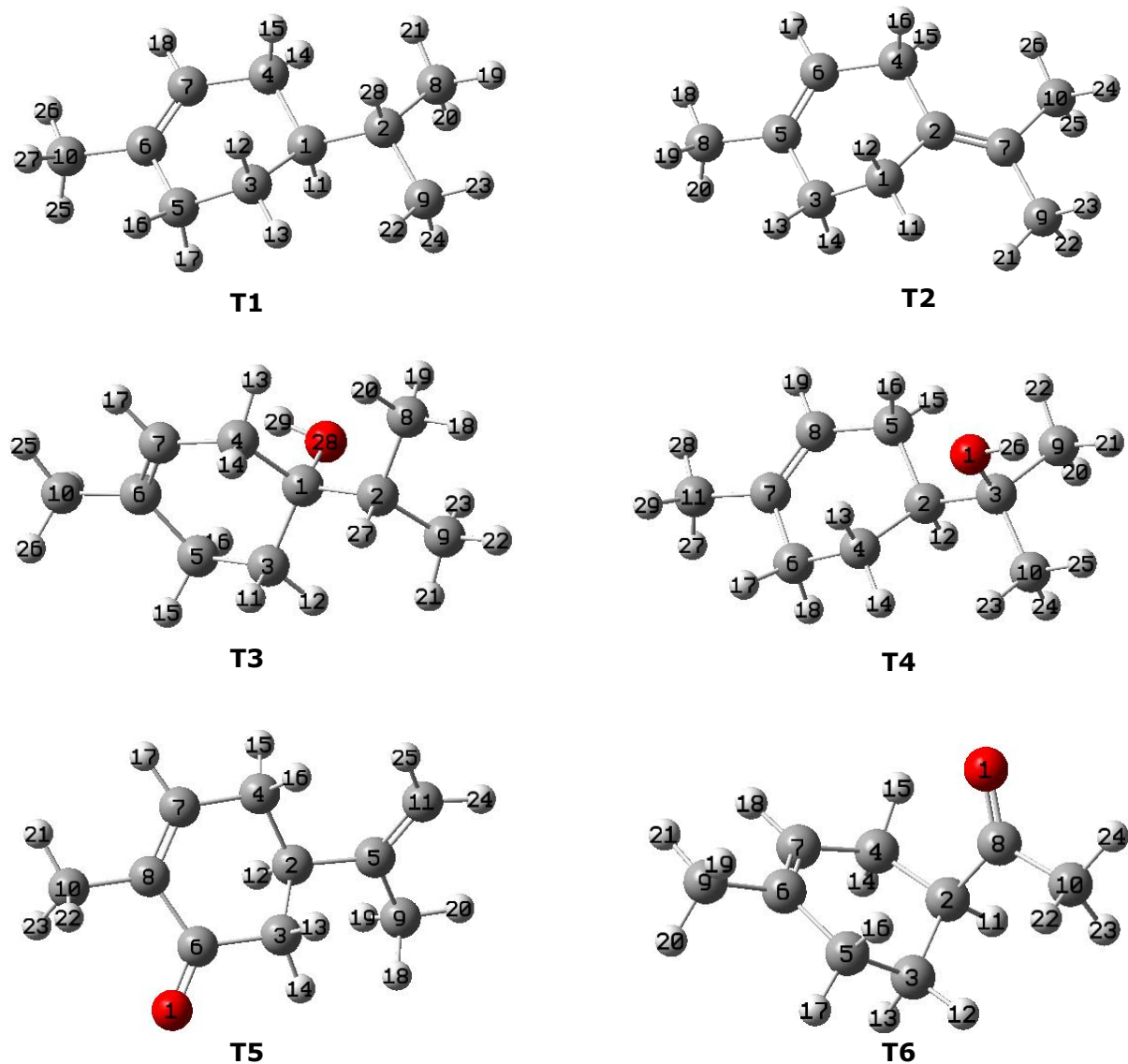
**Figure 1:** The optimized structures of the terpenes.

Conversely, it should be noted from Table 2 that the water solubility of the T6 molecule would be considerably higher than that of other molecules due to the -C=O group located on the aliphatic chain of the compound. Namely, the ESOL (mg/mL x10$^{-1}$) method for the water-solubility of the compounds denoted the order of T6 (46.3)> T5 (5.81)> T3 (2.54)> T1 (2.26)> T4 (2.10)> T2 (0.43), while the Log S (Ali) (mg/mL x10$^{-2}$) gave the following order T6 (692)> T5 (28.5)> T1 (11.0)> T3 (6.75)> T4 (4.95)> T2 (0.880). According to the ALI and ESOL approaches, T2 would have medium-level solubility since the *sp$^2$* hybridized group as the bridge between the aliphatic chain and ring chain probably made the compound more likely to prefer intramolecular interactions instead of acting towards the outer system. On the other hand, the T4 could be more soluble among the molecules according to the SILICOS-IT approach. Although there were different orders of solubility of the compounds, the presence of -C=O and -OH groups in the molecule especially contributed to an increase in the water solubility. Also, the position of these groups on the molecule caused the change of the water solubility of the compıunds. Namely, the solubility of T6 functionalized with the -C=O group on the chain part could be higher than that of the T5, including this group on the ring.

**Table 2:** Physicochemical properties, lipophilicity, and water solubility features.

| Physicochemical properties | T1 | T2 | T3 | T4 | T5 | T6 |
|---|---|---|---|---|---|---|
| Formula | C10H18 | C10H16 | C10H18O | C10H18O | C10H14O | C9H14O |
| Molecular weight (g/mol) | 138.25 | 136.23 | 154.25 g | 154.25 | 150.22 | 138.21 |
| Num. heavy atoms | 10 | 10 | 11 | 11 | 11 | 10 |
| Num. arom. heavy atoms | 0 | 0 | 0 | 0 | 0 | 0 |
| Fraction Csp3 | 0.80 | 0.60 | 0.80 | 0.80 | 0.50 | 0.67 |
| Num. rotatable bonds | 1 | 0 | 1 | 1 | 1 | 1 |
| Num. H-bond acceptors | 0 | 0 | 1 | 1 | 1 | 1 |
| Num. H-bond donors | 0 | 0 | 1 | 1 | 0 | 0 |
| Molar Refractivity | 47.60 | 47.12 | 48.80 | 48.80 | 47.32 | 42.99 |
| TPSA (Å²) | 0.00 | 0.00 | 20.23 | 20.23 | 17.07 | 17.07 |
| | | | | | | |
| *Lipophilicity* | | | | | | |
| Log $P_{o/w}$ (iLOGP) | 2.74 | 2.71 | 2.51 | 2.09 | 2.27 | 2.03 |
| Log $P_{o/w}$ (XLOGP3) | 3.42 | 4.47 | 3.26 | 3.39 | 2.71 | 1.34 |
| Log $P_{o/w}$ (WLOGP) | 3.39 | 3.45 | 2.50 | 2.50 | 2.49 | 2.32 |
| Log $P_{o/w}$ (MLOGP) | 4.29 | 3.27 | 2.30 | 2.30 | 2.10 | 1.89 |
| Log $P_{o/w}$ (SILICOS-IT) | 2.96 | 3.08 | 2.44 | 2.17 | 2.64 | 2.31 |
| Consensus Log $P_{o/w}$ | 3.36 | 3.40 | 2.60 | 2.49 | 2.44 | 1.98 |
| | | | | | | |
| *Water Solubility* | | | | | | |
| Log $S$ (ESOL) | -2.79 | -3.50 | -2.78 | -2.87 | -2.41 | -1.48 |
| Solubility (mg/mL)x10$^{-1}$ | 2.26 | 0.43 | 2.54 | 2.10 | 5.81 | 46.3 |
| Class | S | S | S | S | S | VS |
| | | | | | | |
| Log $S$ (Ali) | -3.10 | -4.19 | -3.36 | -3.49 | -2.72 | -1.30 |
| Solubility (mg/mL)x10$^{-2}$ | 11.0 | 0.880 | 6.75 | 4.95 | 28.5 | 692 |
| Class | S | MS | S | S | S | VS |
| | | | | | | |
| Log $S$ (SILICOS-IT) | -2.25 | -2.46 | -1.91 | -1.69 | -2.16 | -1.76 |
| Solubility (mg/mL) | 0.781 | 0.473 | 1.92 | 3.17 | 1.04 | 2.40 |
| Class | S | S | S | S | S | S |

"TPSA "topological polar surface Area" was calculated based on polar fragments that contributed to the polar surface. S, soluble; MS, moderate soluble; and VS, very soluble."

### 3.3. Absorption, Distribution, Metabolism, and Bioavailability

The ADM-DL study "Absorption, Distribution, Metabolism, Drug-likeness", in essence, is fundamental for the optimization of pharmacokinetic properties and therapeutic efficacy of drug candidates, allowing the design of more effective and safer therapeutic agents. By investigating these factors, it can predict the drug's behavior inside the body, minimize adverse effects, and enhance its therapeutic efficiency. In this respect, the calculated ADM scores and BOILED-EGG and pharmacokinetic radar graphs were represented in Table 3 and Figure 2, respectively.

Accordingly, all compounds were determined in the optimal range (>-5.15 Log unit) in terms of Caco-2 Pe scores that were calculated as T5 (-4.532)< T2 (-4.428)< T6 (-4.369)< T1 (-4.264)< T4 (-4.245)< T3 (-4.191). The MDCK Pe. (x10$^{-5}$) cm/s were determined as T5 (2.8)> T6(2.1)> T1= T3 (2.0)> T4 (1.9)> T2 (1.7), which would display high-level passive permeability (>20x10$^{-6}$ cm/s) for the MDCK Pe. The compound T2 (0.159) could be more potent in terms of the Pgp-inh., whereas the T6 (0.015) could present higher Pgp-subs. potency, relatively. The T3, T4, and T6 (0.004) might display the same

capability for HIA, whereas the T5 (0.006) would have relatively higher potency for HIA. In terms of bioavailability, the T5 and T3 could be promising agents with the $F_{20\%}$ scores at 0.029 and 0.681 (moderate-size), respectively, while the others gave the red alarm about the bioavailability with the scores being determined between 0.897- 0.966. On the other hand, T3 (0.035), T4 (0.19), and T5 (0.003) would denote good bioavailability with the $F_{30\%}$ scores, while T1 (0.873), T2 (0.818), and T6 (0.744) might no bioavailable agent.

The T4 (82.50%), T5 (58.77%), and T6 (80.86%) would present sensible PPB scores (<90%), while T1 (94.62%), T2 (95.54%), and T3 (90.26%) would have higher PPB % scores which might cause the low therapeutic index. Here, the –C=O group located on the ring of the T5 would be more important in the PPB potency than both the -OH and -C=O substitutions on the aliphatic chain. The VD scores for all compounds were calculated in the range of optimal values (0.04-20 L/kg) and found to order of T2 (5.905)> T1(3.887)> T3 (2.457)> T5 (1.650)> T6 (1.650)> T4 (1.497), which implied the compounds would have a sensible volume distribution. Also, T1-T3 would have a BBB Pen. scores in the range of 0.314- 0.576 (in yellow alarm

limits), while the T4-T6 could present the red alarm with BBB Pen. scores in 0.727- 0.971. The portion of the T1 and T2 unbonded in the plasma was calculated with low size at 4.737% and 4.586%, respectively, whereas T3 would be distributed in the plasma as unbonded at a moderate level with a Fu% of 9.940. The T4-T6 could dissolve as unbonded in the plasma at a high level with Fu% changed in 19.13-50.58.

In terms of the metabolism of the compounds, -C=O-modified molecule T6 could have been more promising than the other terpenes, while T4 modified with the -OH group could be a less suitable agent among terpenes. Namely, the CYP1A2 inh. and CYP1A2 subs. values of the compounds were calculated in the orders of T2 (0.925)> T1 (0.757)> T3(0.558)> T6 (0.523)> T5 (0.329)> (0.124) and T6 (0.762)> T1 (0.450)> T5 (0.435)> T3 (0.346)> T2 (0.263)> T4 (0.162), respectively. Also,

CYP2C19 inh. and CYP2C19 subs. scores of the compounds changed in 0.064-0.361 and 0.632-0.790, which could be interpreted to mean that the substrate potency of the compounds was higher than those of the inhibitor potency for CYP2C19.

Similarly, the substrate potencies of the compounds for CYP2C9, CYP2D6, and CYP3A4 were also greater than those of the inhibition potencies. Namely, the scores of inhibitor and substrate potency for CYP2C9 were predicted at 0.468-0.867 and 0.036-0.345, respectively. These results are significant as they provide a nuanced understanding of the interaction of these compounds with various cytochrome P450 enzymes. Understanding these interactions can help predict drug metabolism and potential drug-drug interactions and inform drug design and dosage recommendations.

**Table 3:** Absorption, Distribution, and Metabolism indices.

|  | *T1* | *T2* | *T3* | *T4* | *T5* | *T6* |
|---|---|---|---|---|---|---|
| ***Absorption*** | | | | | | |
| Caco-2 Pe. | -4.264 | -4.428 | -4.191 | -4.245 | -4.532 | -4.369 |
| MDCK Pe. ($\times 10^{-5}$) cm/s | 2 | 1.7 | 2 | 1.9 | 2.8 | 2.1 |
| Pgp-inh. | 0.001 | 0.159 | 0.0 | 0.001 | 0.067 | 0.001 |
| Pgp-subs. | 0.009 | 0.002 | 0.006 | 0.002 | 0.001 | 0.015 |
| HIA | 0.003 | 0.003 | 0.004 | 0.004 | 0.006 | 0.004 |
| $F_{20\%}$ | 0.966 | 0.960 | 0.681 | 0.897 | 0.029 | 0.959 |
| $F_{30\%}$ | 0.873 | 0.818 | 0.035 | 0.19 | 0.003 | 0.744 |
| ***Distribution*** | | | | | | |
| PPB % | 94.62 | 95.54 | 90.26 | 82.50 | 58.77 | 80.86 |
| VD (L/kg) | 3.887 | 5.905 | 2.457 | 1.497 | 1.650 | 1.638 |
| BBB Pen. | 0.561 | 0.314 | 0.576 | 0.727 | 0.968 | 0.971 |
| Fu % | 4.737 | 4.586 | 9.940 | 20.43 | 50.58 | 19.13 |
| ***Metabolism*** | | | | | | |
| CYP1A2 inh. | 0.757 | 0.925 | 0.558 | 0.124 | 0.329 | 0.523 |
| CYP1A2 subs. | 0.450 | 0.263 | 0.346 | 0.162 | 0.435 | 0.762 |
| CYP2C19 inh. | 0.230 | 0.361 | 0.179 | 0.064 | 0.300 | 0.215 |
| CYP2C19 subs. | 0.790 | 0.602 | 0.816 | 0.639 | 0.837 | 0.632 |
| CYP2C9 inh. | 0.290 | 0.345 | 0.089 | 0.052 | 0.052 | 0.036 |
| CYP2C9 subs. | 0.797 | 0.867 | 0.843 | 0.775 | 0.468 | 0.859 |
| CYP2D6 inh. | 0.016 | 0.021 | 0.037 | 0.009 | 0.031 | 0.011 |
| CYP2D6 subs. | 0.351 | 0.254 | 0.252 | 0.243 | 0.608 | 0.845 |
| CYP3A4 inh. | 0.082 | 0.040 | 0.059 | 0.020 | 0.036 | 0.030 |
| CYP3A4 subs. | 0.295 | 0.208 | 0.252 | 0.202 | 0.263 | 0.238 |

"Permeability, Pe; Penetration, Pen, Inhibitor, Inh; Substrate, subs"
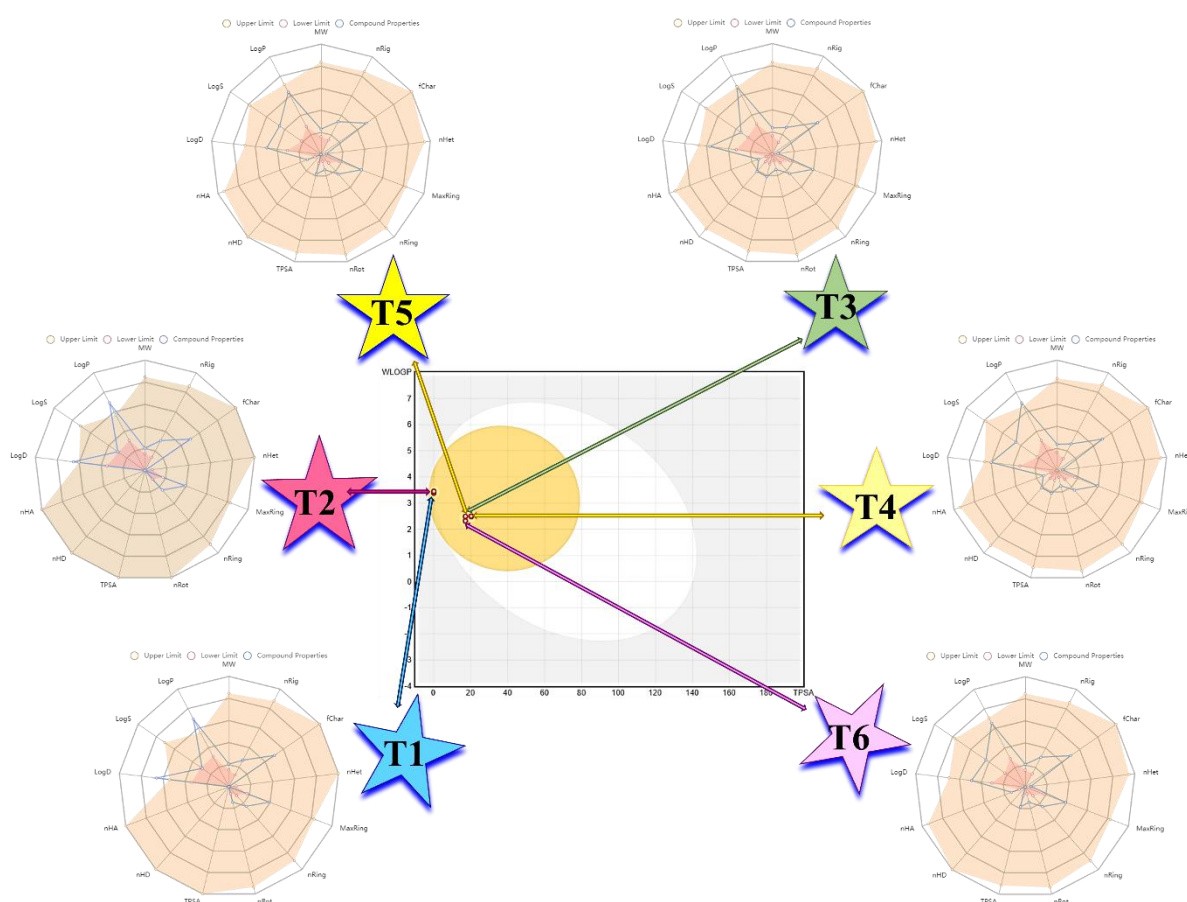
**Figure 2:** BOILED-Egg model and pharmacokinetic radar graphs.

### 3.4. Toxicity Study

A fundamental objective in the field of drug discovery and development is the identification of therapeutic agents that are not only effective but also safe to enhance patient outcomes. This process necessitates an exhaustive assessment of the toxicity of potential drug candidates, as well as an evaluation of their 'drug-likeness'. Computational tools come into play here, providing predictive measures of toxicity scores, which encompass both medicinal and environmental risk factors. These tools also assist in the identification of optimal pharmacokinetic and pharmacodynamic properties, which are key indicators of a drug's behavior within the body. In this context, we have provided the calculated toxicity results in Table 4. These results present a quantitative analysis of potential risk factors associated with each drug candidate, demonstrating their suitability or otherwise for further development.

In considering the possible harmful effect of the compounds T1-T4 and T6 related to the hERG Blockers, H-HT, DILI, AMES, Rat Oral Acute, and FDAMDD (except for T4) the results implied that the compounds would not have a toxic effect on them, due to the calculated scores for all them were close to zero. Here, the FDAMDD indexes of the T4 and T6 were determined at 0.546 and 0.667, which indicated that it could cause a moderate-level toxic effect. Even though the T5 would have been harmful

to FDAMDD (0.874) and H-HT (0.698) at a moderate level, it would not have also been a toxic effect related to the hERG Blockers (0.021), DILI (0.046), AMES (0.013), and Rat Oral Acute (0.027). Furthermore, T6 could cause an unwanted effect with a high possibility on skin (0.905), carcinogenicity (0.902), eye corrosion (0.984) and, irritation (0.988), and respiratory (0.884). Except for T2 (0.597) and T3 (0.698), which would have been an adverse effect at a medium level, the other compounds would also have been adversely in terms of skin sensitization. The carcinogenicity scores of the compıunds were estimated as T4=T6 (0.902)> T2 (0.874)> T5 (0.837)> T1 (0.824)> T3 (0.543); the T3 would have medium-level toxicity, but the others could have toxic potency at a high level. Furthermore, the compounds T1 (0.965), T5 (0.951), and T6 (0.984) implied that they would have undesired effects in terms of eye corrosion, whereas the unwanted effect of the compounds T2 (0.483), T3 (0.664), and T4 (0.696) would be a moderate size. All compounds could irritate the eye due to the high indexes predicted in the range of 0.977-0.992.

Furthermore, the BCF scores of all compounds were computed lower than that of threshold value log BCF< 3.3 (80,81), which meant that they would have no risk in terms of secondary poisoning potential on the environment. From Table 4, the $IGC_{50}$, $LC_{50}FM$, and $LC_{50}DM$ values of the compounds

varied in the following orders of T5 (2.899)> T1 (2.808)> T3 (2.565)> T2 (2.521)> T6 (2.418)> T4 (2.294), T5 (4.263)> T2 (3.501)> T1(3.170)> T6 (2.984)> T3 (2.970)> T4 (2.854), and T2 (4.798)> T1 (4.746)> T3 (4.423)> T5 (4.365)> T6 (4.239)>T4 (3.836), respectively. In recent work, the in-silico toxicity analyses of volatile compounds that are among the components of *Piper acutifolium* have been reported (82); the $IGC_{50}$, $LC_{50}FM$, and $LC_{50}DM$ scores of the terpenes in the investigated essential oil have been predicted in the ranges of 3.080-4.471, 3.674-5.331, and 4.107-5.948, respectively. Although there are some reports that the excessive use of glyphosate caused adverse effects on soils and water (83-85), glyphosate can still be used for comparison purposes due to being considered non-toxic. In this regard, the $IGC_{50}$, $LC_{50}FM$, and $LC_{50}DM$ values of glyphosate have been determined as 2.351, 3.794, and 3.503, respectively (82). Regarding $IGC_{50}$, the studied terpenes, except for T4, could be less toxic than the glyphosate ($IGC_{50}$>2.351). Moreover, the T5 and T6 could be less toxic than glyphosate ($LC_{50}FM$>3.794), while the other terpenes, T1-T4

could be more toxic than glyphosate. Fortunately, all terpenes would be less toxic ($LC_{50}FM$>3.503) than glyphosate.

In view of the Tox21 pathway scores, the T1, T3, T4, and T6 would have no risk in terms of all parameters given in Table 4. Namely, the NR-AR, NR-AR-LBD, and NR-AhR scores of compounds T1-T6 were calculated in the ranges of 0.005-0.096, 0.003-0.008, and 0.011-0.071, respectively, which meant that there would have no any risk potency. The compound T5 could present a moderate-level risk on NR-Aromatase (0.394) and SR-ARE (0.483), whereas the T2 could cause a toxic effect only for NR-ER (0.606). Accordingly, compounds T1, T3, T4, and T6 demonstrated negligible risk based on various parameters, including low NR-AR, NR-AR-LBD, and NR-AhR scores. However, compound T5 indicated a moderate risk level for NR-Aromatase and SR-ARE, and T2 posed a potential toxicity risk for NR-ER. Despite the majority of compounds showing minimal risk, T5 and T2 should have needed further examination due to their potential risk factors.

**Table 4:** Toxicity scores.

|  | *T1* | *T2* | *T3* | *T4* | *T5* | *T6* |
|---|---|---|---|---|---|---|
| ***Medicinal*** |  |  |  |  |  |  |
| hERG Blockers | 0.022 | 0.020 | 0.015 | 0.010 | 0.021 | 0.017 |
| H-HT | 0.185 | 0.213 | 0.075 | 0.138 | 0.698 | 0.362 |
| DILI | 0.241 | 0.185 | 0.054 | 0.039 | 0.046 | 0.219 |
| AMES Tox. | 0.013 | 0.004 | 0.006 | 0.005 | 0.013 | 0.053 |
| Rat Oral Acute Tox. | 0.018 | 0.009 | 0.017 | 0.020 | 0.027 | 0.082 |
| FDAMDD | 0.067 | 0.032 | 0.020 | 0.546 | 0.874 | 0.667 |
| Skin Sens. | 0.889 | 0.597 | 0.698 | 0.726 | 0.940 | 0.905 |
| Carcinogencity | 0.824 | 0.874 | 0.543 | 0.902 | 0.837 | 0.902 |
| Eye Corrosion | 0.965 | 0.483 | 0.664 | 0.696 | 0.951 | 0.984 |
| Eye Irritation | 0.982 | 0.977 | 0.985 | 0.984 | 0.992 | 0.988 |
| Respiratory Tox. | 0.053 | 0.020 | 0.026 | 0.083 | 0.889 | 0.884 |
|  |  |  |  |  |  |  |
| **Environmental** |  |  |  |  |  |  |
| BCF | 2.383 | 2.135 | 1.147 | 0.748 | 0.754 | 0.660 |
| $IGC_{50}$ | 2.808 | 2.521 | 2.565 | 2.294 | 2.899 | 2.418 |
| $LC_{50}FM$ | 3.170 | 3.501 | 2.970 | 2.854 | 4.263 | 2.984 |
| $LC_{50}DM$ | 4.746 | 4.798 | 4.423 | 3.836 | 4.365 | 4.239 |
|  |  |  |  |  |  |  |
| **Tox21 Pathway** |  |  |  |  |  |  |
| NR-AR | 0.009 | 0.013 | 0.034 | 0.005 | 0.014 | 0.096 |
| NR-AR-LBD | 0.003 | 0.003 | 0.003 | 0.004 | 0.004 | 0.008 |
| NR-AhR | 0.012 | 0.026 | 0.011 | 0.018 | 0.071 | 0.015 |
| NR-Aromatase | 0.004 | 0.006 | 0.009 | 0.005 | 0.394 | 0.007 |
| NR-ER | 0.124 | 0.606 | 0.064 | 0.119 | 0.079 | 0.176 |
| NR-ER-LBD | 0.201 | 0.232 | 0.005 | 0.007 | 0.013 | 0.038 |
| NR-PPAR-gamma | 0.003 | 0.005 | 0.004 | 0.003 | 0.004 | 0.005 |
| SR-ARE | 0.016 | 0.021 | 0.024 | 0.021 | 0.483 | 0.025 |
| SR-ATAD5 | 0.003 | 0.004 | 0.003 | 0.004 | 0.011 | 0.009 |
| SR-HSE | 0.075 | 0.274 | 0.028 | 0.022 | 0.222 | 0.028 |
| SR-MMP | 0.016 | 0.013 | 0.032 | 0.021 | 0.038 | 0.015 |
| SR-p53 | 0.003 | 0.007 | 0.008 | 0.003 | 0.063 | 0.006 |

"The abbreviations are defined as: Tox, Toxicity; sens, Sensitization; BCF, the unit of bioconcentration factors, IGC50, LC50FM, and LC50DM is given in -Log10[(mg/L)/(1000xMW)]."

## 3.5. NBO study

The NBO method is also fairly used to estimate the key intramolecular interactions that have a critical role in lowering the stabilization energy and thus evaluating the chemical behavior of the molecular systems (86-88). Here, the selected interactions of terpenes were given in Table 5; full data of interactions was given in Table S1 (suppl. data).

Here, it should be noted that the studied systems are not aromatic, and mainly, the possible interactions would have related to the less familiar interactions such as anomeric, cieplak, negative hyperconjugation, etc. Among the terpenes, the resonance interaction was only determined for the T5 structure. Namely, the resonances of π O7-C8 (ED$_i$=1.86177e)→ π* C1-C6 (ED$_j$=0.13989e) and π O1-C6 (ED$_i$=1.97064e)→ π* C7-C8 (ED$_j$=0.08951e) for T5 was predicted with the energies of 20.26 and 5.96 kcal/mol, respectively. Furthermore, the anomeric interactions would play a remarkable role in stabilizing the T5 molecule: the charge transfers from LP (2) O1 (ED$_i$=1.89090e) to unfilled orbitals σ* C3-C6 (ED$_j$=0.05893e) and σ* C6-C8 (EDj=0.07124e) was calculated with the energies of 19.67 and 18.66 kcal/mol, respectively. In addition, the energy of the hyperconjugation σ C3-H13 (ED$_i$=1.95935e)→ π* O1-C6 (ED$_j$=0.13989e) was calculated as 6.90 kcal/mol. From Table S1 (see suppl. data), the other hyperconjugation energies for the T5 compound were calculated in the range of 2.01-5.29 kcal/mol. Also, the negative hyperconjugations (π→ σ*) for T5 could be remarkable in lowering the stabilization energy predicted in the range of 2.07-3.51 kcal/mol (Table S1). Moreover, the cieplak interactions occurred in the T5 molecule σ C7-H17→ σ* C6-C8 (E$^{(2)}$= 6.31 kcal/mol), σ C11-H24→ σ* C2-C5 (E$^{(2)}$= 7.82 kcal/mol), and σ C11-H25→ σ* C5-C9 (E$^{(2)}$= 6.96 kcal/mol) would have responsibility on the stabilization of the molecule. For the molecule T5, the energies of the other cieplak interactions would be in the range of 2.84-4.56 kcal/mol. From Table 5, the highest portion of the lowering the stabilization for T6 would source from the anomeric interactions LP (2) O1→ σ* C2-C8 (ED$_j$=0.07531e) and LP (2) O1→ σ* C8-C10 (ED$_j$=0.05710e) with the E$^{(2)}$ of 20.63 and 20.51 kcal/mol, respectively. Furthermore, the highest energy hyperconjugation for T6 was found to be σ C2-H11→ π* O1-C8 (E$^{(2)}$= 6.41 kcal/mol) and C10-H22 → π* O1-C8 (E$^{(2)}$= 6.27 kcal/mol), and the orbital occupancies of them were with the remarkable. Energies of the other hyperconjugative interactions were calculated in the range of 2.70-4.71 kcal/mol (Table S1). Moreover, the negative σ-conjugations would have an important role in lowering the energy; the energies of the interactions π C6-C7 (ED$_i$=1.93464e)→ σ* C5-H16 (ED$_j$=0.02157e) and π C6-C7→ σ* C4-H15 (ED$_j$=0.01707e) for T6 were estimated in 3.75 and 2.05 kcal/mol, respectively. The calculated energies for the cieplak interactions were changed in the range of 2.55-7.25 kcal/mol; the highest energy interaction was σ C7-H18→ σ* C5-C6, and the lowest energy one would be σ C2-C4→ σ* C8-C10.

Moreover, the T3 and T4 molecules functionalized with the -OH group on the ring exhibited that the conjugative interactions could have a critical role in terms of stability. For T3, the hyperconjugations σ C5-H16 (ED$_i$=1.96644e)→ π* C6-C7 (ED$_j$=0.09324e) and σ C4-H14 (ED$_i$=1.96389e)→ π* C6-C7 (ED$_i$=1.96389e) were predicted with the energies of 5.10 and 4.46 kcal/mol, respectively. On the other hand, the energies of the negative σ-conjugations for the compounds T3 and T4 were determined in the ranges of 2.22-3.97 kcal/mol and 2.12-3.75 kcal/mol, respectively. The interaction σ C7-H17→ σ* C5-C6 for T3 was estimated with the energy of 7.04 kcal/mol, whereas the corresponding interaction for T4 was predicted as σ C8-H19→ σ* C6-C7 with the same energy. Similarly, the same cieplak interaction for T1 and T2 molecules would be responsible for the stabilization of the system with the same energy (7.04 kcal/mol).

## 3.6. Atomic Charges

The prediction of the atomic charges (74,75,89) also provides a useful viewpoint in the evaluation of the local reactivity site (s) of the molecular systems. Herein, the calculated atomic charges of the compounds obtained from MPA and NPA approaches were summarized in Table 6; the whole data was given in Tables S2 and S3, respectively.

For the T1 and T2 without heteroatom, the lowest charges were determined for the Cs of the methyl groups due to the existence of the electron-donating Hs. Namely, the charges of the C8, C9, and C10 atoms of T1 were predicted as -0.270782, -0.264074, and -0.252332 by MPA and -0.57090, -0.56977, and -0.58350 by NPA methods. Furthermore, the charges of the atoms C8, C9, and C10 for T2 by MPA and NPA methods were found to be -0.251532, -0.256386, -0.255652, and -0.58311, -0.58721, -0.58941, respectively. According to the results of the MPA approach, the charges of all C atoms for T1 and T2 were found to be negative values, while the C atoms' charges for T3 were calculated in positive value except for C7 (-0.051884). On the other hand, the NPA method depends on the NBO method, which considers the non-covalent interactions in the relevant molecular system and thus reveals a different charge distribution. Especially, the presence of the electronegative oxygen atom makes the charge distribution on the surface different from MPA. Namely, the C1 charge for T3 by MPA and NPA was determined as 0.401289 and 0.33652, respectively; the non-covalent interactions aforementioned in the NBO section would be responsible for the decrease of the charge density on the C1 atom. MPA calculated the partial charge of the O28 atom of T3 at -0.593646, which was bigger than that of -0.77131 predicted by NPA, as expected from the basics of this approach that care of the non-covalent interactions.

Furthermore, O1 charge for T4-T6 molecules was estimated by the MPA at -0.401483, -0.302913, and -0.293275, respectively, while it was determined by

the NPA method as -0.76279, -0.55670, and -0.55395. For all terpenes, the O atom that was a part of the alcohol or ketone group exhibited more negative charge distribution as an indicator of the electron abundance region, as expected. Also, the H' charge of the –OH group for T3 and T4 were determined by MPA as 0.234756 (H29) and 0.233889 (H26), respectively, while NPA estimated them as 0.45585 and 0.44580. On the other hand, the C6 (T5) and C8 (T6) charges were estimated by the MPA method at 0.201871 and 0.221130, respectively, whereas the NPA method revealed these charges at 0.56430 and 0.60869, respectively. For both methods, the Hs' charges for all terpenes were determined to be higher than zero, as expected from the electropositive nature of the atom (Tables S2 and S3).

**Table 5.** The second-order perturbative energy analyze, at B3LYP/6-311G(d,p) in gas phase.

| Donor(i) | $ED_i/e$ | Acceptor (j) | $ED_j/e$ | $E^{(2)}$/ kcalmol$^{-1}$ | E(j)-E(i)/ a.u | F(i.j)/ a.u |
|---|---|---|---|---|---|---|
| **T1** | | | | | | |
| σ C1-C3 | 1.97439 | σ* C2-C8 | 0.01470 | 2.29 | 0.97 | 0.042 |
| σ C4-H14 | 1.97091 | π* C6-C7 | 0.09146 | 2.71 | 0.55 | 0.035 |
| σ C5-H17 | 1.96779 | π* C6-C7 | 0.09146 | 4.84 | 0.55 | 0.047 |
| π C6-C7 | 1.93549 | σ* C4-H14 | 0.01578 | 2.00 | 0.68 | 0.033 |
| | | σ* C4-H15 | 0.02255 | 3.84 | 0.66 | 0.045 |
| σ C7-H18 | 1.97579 | σ* C5-C6 | 0.02967 | 7.04 | 0.93 | 0.072 |
| | | | | | | |
| **T2** | | | | | | |
| σ C1-C3 | 1.97198 | π* C2-C7 | 0.10885 | 2.17 | 0.67 | 0.035 |
| π C2-C7 | 1.91864 | σ* C4-H16 | 0.02484 | 3.84 | 0.65 | 0.045 |
| σ C4-H16 | 1.95867 | π* C2-C7 | 0.10885 | 4.89 | 0.56 | 0.048 |
| π C5-C6 | 1.93711 | σ* C4-H15 | 0.01574 | 2.11 | 0.68 | 0.034 |
| σ C6-H17 | 1.97582 | σ* C3-C5 | 0.02910 | 7.04 | 0.93 | 0.072 |
| | | | | | | |
| **T3** | | | | | | |
| σ C1-C3 | 1.97260 | σ* C2-C8 | 0.01502 | 2.28 | 0.98 | 0.042 |
| σ C4-H13 | 1.97025 | π* C6-C7 | 0.09324 | 2.45 | 0.55 | 0.033 |
| σ C5-H16 | 1.96644 | π* C6-C7 | 0.09324 | 5.10 | 0.55 | 0.048 |
| π C6-C7 | 1.93482 | σ* C4-H14 | 0.02093 | 3.97 | 0.67 | 0.047 |
| | | σ* C5-H15 | 0.01658 | 2.22 | 0.68 | 0.035 |
| σ C7-H17 | 1.97622 | σ* C5-C6 | 0.02971 | 7.04 | 0.93 | 0.072 |
| LP (2) O28 | 1.95436 | σ* C1-C3 | 0.04278 | 7.80 | 0.67 | 0.065 |
| | | | | | | |
| **T4** | | | | | | |
| σ C5-C8 | 1.97669 | σ* C2-C3 | 0.04022 | 2.22 | 0.98 | 0.042 |
| σ C5-H15 | 1.97058 | π* C7-C8 | 0.09223 | 2.77 | 0.55 | 0.036 |
| σ C6-H18 | 1.96830 | π* C7-C8 | 0.09223 | 4.84 | 0.56 | 0.047 |
| π C7-C8 | 1.93603 | σ* C5-H15 | 0.01567 | 2.03 | 0.67 | 0.033 |
| | | σ* C6-H18 | 0.02139 | 3.75 | 0.66 | 0.045 |
| σ C8-H19 | 1.97564 | σ* C6-C7 | 0.02968 | 7.04 | 0.93 | 0.072 |
| LP (2) O1 | 1.95531 | σ* C3-C9 | 0.03255 | 5.37 | 0.66 | 0.053 |
| | | σ* C3-C10 | 0.03294 | 5.98 | 0.67 | 0.056 |
| | | | | | | |
| **T5** | | | | | | |
| π O1-C6 | 1.97064 | σ* C3-H13 | 0.01579 | 2.07 | 0.76 | 0.036 |
| σ C3-H13 | 1.95935 | π* O1-C6 | 0.13989 | 6.90 | 0.52 | 0.055 |
| σ C4-H15 | 1.97289 | π* C7-C8 | 0.08951 | 2.01 | 0.86 | 0.047 |
| π C7-C8 | 1.86177 | π* O1-C6 | 0.13989 | 20.26 | 0.30 | 0.070 |
| σ C11-H24 | 1.98240 | σ* C2-C5 | 0.03618 | 7.82 | 0.94 | 0.077 |
| LP (2) O1 | 1.89090 | σ* C3-C6 | 0.05893 | 19.67 | 0.65 | 0.102 |
| | | σ* C6-C8 | 0.07124 | 18.66 | 0.71 | 0.104 |
| | | | | | | |
| **T6** | | | | | | |
| σ C2-C4 | 1.97443 | σ* C8-C10 | 0.05710 | 2.55 | 0.98 | 0.045 |
| σ C2-H11 | 1.95033 | π* O1-C8 | 0.08421 | 6.41 | 0.51 | 0.052 |
| σ C5-H17 | 1.97195 | π* C6-C7 | 0.09008 | 2.70 | 0.56 | 0.035 |
| π C6-C7 | 1.93464 | σ* C4-H15 | 0.01707 | 2.05 | 0.69 | 0.034 |
| | | σ* C5-H16 | 0.02157 | 3.75 | 0.66 | 0.045 |
| σ C7-H18 | 1.97498 | σ* C5-C6 | 0.02978 | 7.25 | 0.92 | 0.073 |
| LP (2) O1 | 1.88596 | σ* C2-C8 | 0.07531 | 20.63 | 0.65 | 0.104 |
| | | σ* C8-C10 | 0.05710 | 20.51 | 0.64 | 0.104 |

**Table 6:** The selected atomic charges of terpenes in gas phase.

| | *T1* | *T2* | *T3* | | | *T4* | *T5* | *T6* |
|---|---|---|---|---|---|---|---|---|
| **MPA** | | | | | | | | |
| C1 | -0.189984 | -0.200904 | 0.401289 | | O1 | -0.401483 | -0.302913 | -0.293275 |
| C2 | -0.185028 | -0.102881 | 0.118172 | | C2 | -0.184721 | -0.222480 | -0.265890 |
| C3 | -0.190141 | -0.166907 | 0.018783 | | C3 | -0.014241 | -0.187501 | -0.220248 |
| C4 | -0.150511 | -0.118736 | 0.024100 | | C4 | -0.182113 | -0.159843 | -0.145180 |
| C5 | -0.170717 | -0.115804 | 0.077870 | | C5 | -0.147422 | -0.101527 | -0.189606 |
| C6 | -0.124793 | -0.111715 | 0.054923 | | C6 | -0.173012 | 0.201871 | -0.107730 |
| C7 | -0.094971 | -0.141937 | -0.051884 | | C7 | -0.125081 | -0.080330 | -0.084984 |
| C8 | -0.270782 | -0.251532 | 0.025376 | | C8 | -0.094835 | -0.130282 | 0.221130 |
| C9 | -0.264074 | -0.256386 | 0.024556 | | C9 | -0.240234 | -0.239866 | -0.252887 |
| C10 | -0.252332 | -0.255652 | 0.074607 | | C10 | -0.225768 | -0.229155 | -0.301834 |
| O28 | | | -0.593646 | | C11 | -0.252679 | -0.173070 | 0.136967 |
| H29 | | | 0.234756 | | H26 | 0.233889 | | |
| | | | | | | | | |
| **NPA** | | | | | | | | |
| C1 | -0.20078 | -0.39032 | 0.33652 | | O1 | -0.76279 | -0.55670 | -0.55395 |
| C2 | -0.18840 | -0.01097 | -0.21065 | | C2 | -0.22279 | -0.22540 | -0.29387 |
| C3 | -0.37225 | -0.39335 | -0.40359 | | C3 | 0.33880 | -0.46133 | -0.36614 |
| C4 | -0.40755 | -0.42643 | -0.44550 | | C4 | -0.37461 | -0.41905 | -0.40852 |
| C5 | -0.39956 | -0.00110 | -0.41055 | | C5 | -0.41211 | 0.01828 | -0.41049 |
| C6 | 0.00179 | -0.19087 | -0.00048 | | C6 | -0.39879 | 0.56430 | -0.00448 |
| C7 | -0.19484 | -0.00311 | -0.20882 | | C7 | -0.00080 | -0.10130 | -0.18752 |
| C8 | -0.57090 | -0.58311 | -0.57416 | | C8 | -0.19188 | -0.11580 | 0.60869 |
| C9 | -0.56977 | -0.58721 | -0.57217 | | C9 | -0.60281 | -0.59115 | -0.58307 |
| C10 | -0.58350 | -0.58941 | -0.58492 | | C10 | -0.60096 | -0.58472 | -0.67271 |
| O28 | | | -0.77131 | | C11 | -0.58303 | -0.39175 | 0.21764 |
| H29 | | | 0.45585 | | H26 | 0.44580 | | |

### 3.7. FMO (Frontier Molecular Orbital) Analysis and MEP (Molecular Electrostatic Potential)

Nowadays, global reactivity descriptors play an inevitable role in computational chemistry and molecular physics. They provide a quantitative means to evaluate the overall reactivity of a molecular system, giving invaluable insights into its behavior and interactions with other molecules (86-88, 90,91). Thus, they help to design new chemical compounds and predict potential outcomes in drug design and other chemical synthesis processes.

By using the *I* and *A* values given in Table 7, the calculated reactivity indices of T1-T6 changed in the gas phase in the following orders. According to ΔE order, T1 would tend to interact with the external system rather than intramolecular actions, whereas T5 could prefer intramolecular interactions more than acting with the outer system. On the other hand, the T5 would be more stable electronically than the others, and vice versa for T4, depending on the μ. T1 was predicted to be the hardest molecule, while the soft compound would be T5. ω scores denoted that T5 could have bigger electrophilicity than the others and vice versa for T1 and T4. In addition, T5 would present more electron-donating or electron-accepting potency than the other compounds, and vice versa for T4. Supportingly, the charge transfer potency of T5 could be bigger than the others, and vice versa for T4. Moreover, the T1 would have gained more stability by the back donation than the others, and T5 was determined to have gained less stability relatively.

*H (-I) (eV): T2 (-6.091)> T4 (-6.209)> T1 (-6.324)> T6 (-6.385)> T3 (-6.619)> T5 (-6.667)*
*L (-A) (eV): T1 (0.652)> T4 (0.643)> T2 (0.514)> T3 (0.344)> T5 (-1.478)> T6 (-0.516)*
ΔE (L-H) (eV): T1 (6.976)> T3 (6.963)> T4 (6.852)> T2 (6.605)> T6 (5.869)> T5 (5.189)
μ (eV): T5 (-4.073)< T6 (-3.451)< T3 (-3.138)< T1 (-2.836)< T2 (-2.788)< T4 (-2.783)
η (eV): T1 (3.488)> T3 (3.482)> T4(3.426)> T2 (3.303)> T6 (2.934)> T5 (2.594)
ω (eV): T5 (0.117)> T6 (0.075)> T3 (0.052)> T2 (0.043)> T1=T4 (0.042)
ω+ (au): T5 (0.055)> T6 (0.025)> T3 (0.010)>T2 (0.007)> T1= T4 (0.006)
ω- (au): T5 (0.204)> T6 (0.151)> T3 (0.126)> T1 (0.111)> T2 (0.110)> T4 (0.108)

$\Delta N_{max.}$ (eV): T5 (1.570)> T6 (1.176)> T3 (0.901)> T2 (0.844)> T1 (0.813)> T4 (0.812)
$\Delta E_{back.}$ (eV): T1 (-0.872)< T3 (-0.870)< T4 (-0.856)< T2(-0.826)< T6 (-0.734)< T5 (-0.649)

In the water phase, the $\Delta E$, $\mu$, $\eta$, $\omega$, $\omega+$, and $\Delta E_{back}$. Indexes gave the same order as those in the gas phase. On the other hand, $\omega-$ (au) values changed as T5 (0.212)> T6 (0.157)> T3 (0.122)> T1=T2=T4 (0.113); here, the electron donating potencies of T1, T2, and T4 approximately were calculated close to each other. Moreover, $\Delta N_{max.}$ (eV) values varied in the order of T5 (1.601)> T6 (1.216)> T3 (0.877)> T2 (0.858)> T4 (0.827)> T1 (0.826); the T1 would gain the less stability via back donation comparison to other compounds.

Over the years, FMO and MEP graphs have established themselves as indispensable theoretical tools in the realm of computational chemistry. These plots enable a visual examination of the electronic structure and reactivity of molecules,

thereby trying to light on their complex behavior and characteristics. From Figure 3, the HOMO density for all molecules was concentrated around the double bonds, whereas it for T3-T6 was distributed on neighboring bonds around the oxygen atom. Moreover, the LUMO for T1 and T3-T5 expanded on the hexene ring mainly, while it for T6 expanded over the aliphatic part mainly and on the ring slightly and, the LUMO for T2 covered all molecular surfaces. For T4, the red color as a function of the negative electrostatic potential (V<0) appeared on the oxygen atom and double bonds for the electrophiles, whereas the blue color (V>0) was seen on the H atom for the nucleophiles. For T1 and T2, the area around the double bond was covered in red.

**Table 7:** The chemical reactivity indices

|  |  | T1 | T2 | T3 | T4 | T5 | T6 |
|---|---|---|---|---|---|---|---|
| **Gas** | H (-I) (eV) | -6.324 | -6.091 | -6.619 | -6.209 | -6.667 | -6.385 |
|  | L (-A) (eV) | 0.652 | 0.514 | 0.344 | 0.643 | -1.478 | -0.516 |
|  | $\Delta E$ (L-H) (eV) | 6.976 | 6.605 | 6.963 | 6.852 | 5.189 | 5.869 |
|  | $\mu$ (eV) | -2.836 | -2.788 | -3.138 | -2.783 | -4.073 | -3.451 |
|  | $\eta$ (eV) | 3.488 | 3.303 | 3.482 | 3.426 | 2.594 | 2.934 |
|  | $\omega$ (eV) | 0.042 | 0.043 | 0.052 | 0.042 | 0.117 | 0.075 |
|  | $\omega+$ (au) | 0.006 | 0.007 | 0.010 | 0.006 | 0.055 | 0.025 |
|  | $\omega-$ (au) | 0.111 | 0.110 | 0.126 | 0.108 | 0.204 | 0.151 |
|  | $\Delta N_{max.}$ (eV) | 0.813 | 0.844 | 0.901 | 0.812 | 1.570 | 1.176 |
|  | $\Delta E_{back.}$ (eV) | -0.872 | -0.826 | -0.870 | -0.856 | -0.649 | -0.734 |
|  |  |  |  |  |  |  |  |
| **Water** | H (-I) (eV) | -6.385 | -6.170 | -6.551 | -6.361 | -6.805 | -6.442 |
|  | L (-A) (eV) | 0.608 | 0.471 | 0.430 | 0.602 | -1.571 | -0.629 |
|  | $\Delta E$ (L-H) (eV) | 6.993 | 6.641 | 6.982 | 6.963 | 5.234 | 5.813 |
|  | $\mu$ (eV) | -2.888 | -2.850 | -3.061 | -2.879 | -4.188 | -3.535 |
|  | $\eta$ (eV) | 3.497 | 3.320 | 3.491 | 3.481 | 2.617 | 2.906 |
|  | $\omega$ (eV) | 0.044 | 0.045 | 0.049 | 0.044 | 0.123 | 0.079 |
|  | $\omega+$ (au) | 0.007 | 0.008 | 0.009 | 0.007 | 0.058 | 0.027 |
|  | $\omega-$ (au) | 0.113 | 0.113 | 0.122 | 0.113 | 0.212 | 0.157 |
|  | $\Delta N_{max.}$ (eV) | 0.826 | 0.858 | 0.877 | 0.827 | 1.601 | 1.216 |
|  | $\Delta E_{back.}$ (eV) | -0.874 | -0.830 | -0.873 | -0.870 | -0.654 | -0.727 |
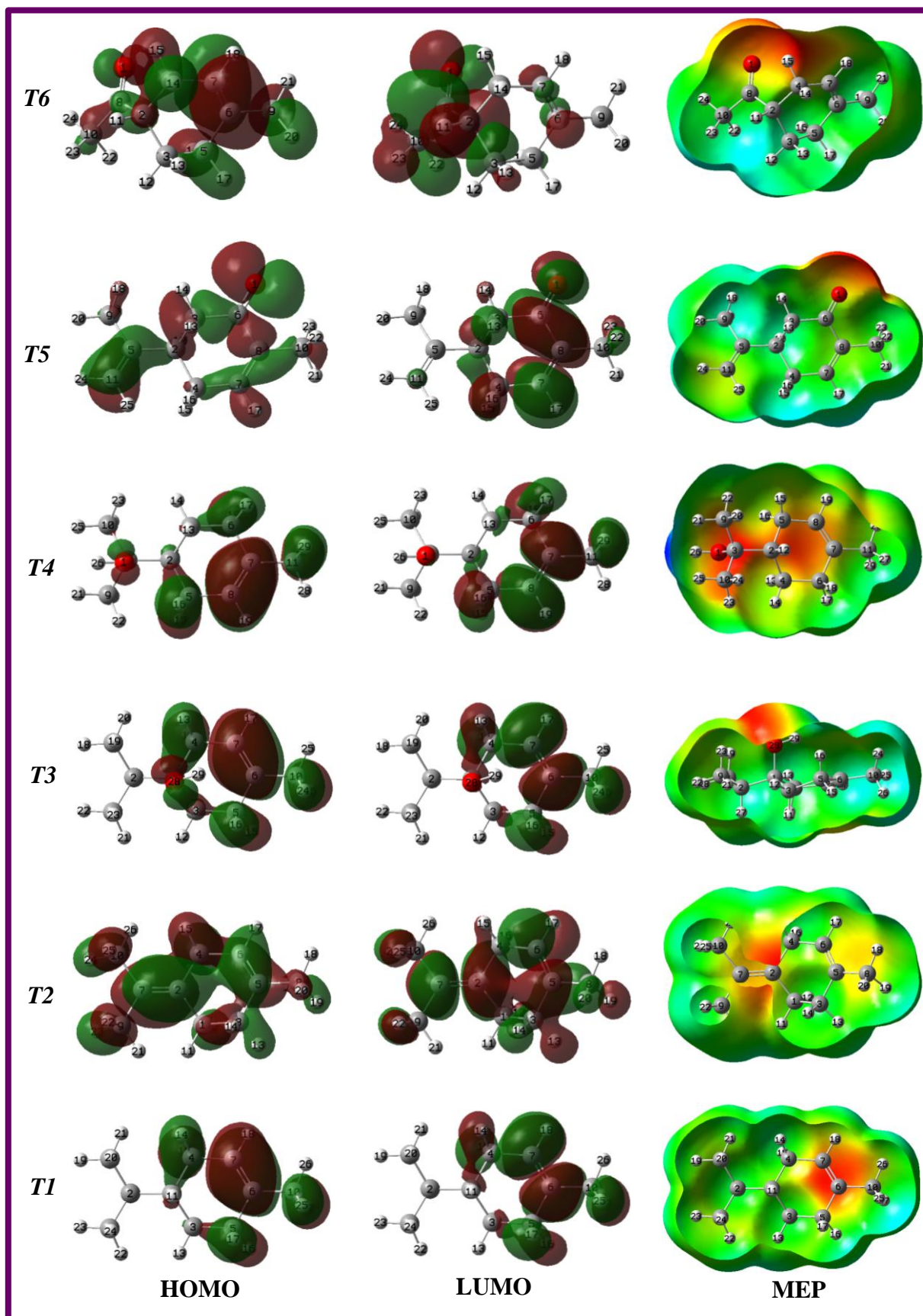
**Figure 3:** HOMO& LUMO, and MEP visualizations of T1-T6.

## 4. CONCLUSION

In this work, the DFT/DFT/B3LYP/6-311G** level computations were performed to predict the physicochemical and electronic characteristics of the terpenes T1-T6. In this regard, the FMO and MEP analyses were used to predict the possible reactivity direction and site(s). Moreover, the NBO analyses and atomic charges of the compounds were determined to evaluate the intramolecular interactions and charge distribution on the whole surface, which would be important to provide insight into the possible bioactivity, drug-likeness, toxicity, etc. In conclusion, the key points obtained from the computational tools of this work can be summarized as follows:

# The T1 and T2 molecules were more lipophilic than the other molecules, whereas T5 and T6 molecules were found to be less lipophilic.
# T5 and T6 functionalized with the -C=O group's most soluble compounds, while T2 was the less soluble one among the compounds, depending on results obtained from ALI and ESOL approaches.
# VD (L/kg) values of all compounds were estimated in the optimal range of 0.04-20 L/kg, which would be very important in terms of the distribution of each of them.
# NBO analyses revealed that cieplak (σ→ σ*) interactions for T1-T4 would be important to lowering the stabilization energy, predicted at 7.04 kcal/mol. In contrast, the resonance (π→ π*) interaction for T5 was predicted with the energy of 20.26 kcal/mol which was the highest contributed interaction to E(2).
# FMO analyses indicated that T5 (0.204 au) could prefer electron donation more than the other terpenes, while T4 (0.108 au) would prefer electron donation less than the others.
# MEP plots implied that the surround of the oxygen atom for T3-T6 molecules would be the electron-rich region for the electrophiles, whereas the around of the double bonds of T1 and T2 would be possible sites for the electrophiles.
# The NPA approach revealed that the atomic charge of the O1 atom of terpenes T4-T6 was predicted at -0.76279, -0.55670, and -0.55395, whereas the O28 atom' charge was found to be at -0.77131, remarkable.

It is hoped that the findings derived from this study will shed light on the interplay between ADM attributes, toxicity, and electronic structure, thereby contributing to the discovery, development, and refinement of prospective pharmaceutical agents.

## 5. ACKNOWLEDGMENTS

## 6. REFERENCES

1. McGarvey DJ, Croteau R. Terpenoid metabolism. Plant Cell. 1995;7(7):1015-1026. Available from: <URL>.

2. Masyita A, Sari RM, Astuti AD, Yasir B, Rumata NR, Emran TB, et al. Terpenes and terpenoids as main bioactive compounds of essential oils, their roles in human health and potential application as natural food preservatives. Food Chem X. 2022;13:100217. Available from: <URL>.

3. Brahmkshatriya PP, Brahmkshatriya PS. Terpenes: Chemistry, Biological Role, and Therapeutic Applications. In: Ramawat K, Mérillon JM, eds. Natural Products. Berlin, Heidelberg: Springer; 2013. Available from: <URL>.

4. Pichersky E, Gershenzon J. The formation and function of plant volatiles: perfumes for pollinator attraction and defense. Curr Opin Plant Biol. 2002;5(3):237-243. Available from: <URL>.

5. Bakkali F, Averbeck S, Averbeck D, Idaomar M. Biological effects of essential oils – A review. Food Chem Toxicol. 2008;46(2):446-475. Available from: <URL>.

6. Del Prado-Audelo ML, Cortés H, Caballero-Florán IH, González-Torres M, Escutia-Guadarrama L, Bernal-Chávez SA, et al. Therapeutic Applications of Terpenes on Inflammatory Diseases. Front Pharmacol. 2021;12:704197. Available from: <URL>.

7. Wen CC, Kuo YH, Jan JT, Liang PH, Wang SY, Liu HG, et al. Specific plant terpenoids and lignoids possess potent antiviral activities against severe acute respiratory syndrome coronavirus. J Med Chem. 2007;50(17):4087-4095. Available from: <URL>.

8. Guimarães AC, Meireles LM, Lemos MF, Guimarães MCC, Endringer DC, Fronza M, et al. Antibacterial Activity of Terpenes and Terpenoids Present in Essential Oils. Molecules. 2019;24(13):2471. Available from: <URL>.

9. Ansari IA, Akhtar MS. Current Insights on the Role of Terpenoids as Anticancer Agents: A Perspective on Cancer Prevention and Treatment. In: Swamy M, Akhtar M, eds. Natural Bio-active Compounds. Singapore: Springer; 2019. Available from: <URL>.

10. Kamran S, Sinniah A, Abdulghani MAM, Alshawsh MA. Therapeutic Potential of Certain Terpenoids as Anticancer Agents: A Scoping Review. Cancers. 2022;14(5):1100. Available from: <URL>.

11. Fan M, Yuan S, Li L, Zheng J, Zhao D, Wang C, et al. Application of Terpenoid Compounds in Food and Pharmaceutical Products. Fermentation. 2023;9(2):119. Available from: <URL>.

12. Gutiérrez-del-Río I, López-Ibáñez S, Magadán-Corpas P, Fernández-Calleja L, Pérez-Valero Á, Tuñón-Granda M, et al. Terpenoids and Polyphenols as Natural Antioxidant Agents in Food Preservation. Antioxidants. 2021;10(8):1264. Available from: <URL>.

13. Yang W, Chen X, Li Y, Guo S, Wang Z, Yu X. Advances in Pharmacological Activities of Terpenoids. Nat Prod Commun. 2020;15(3):1-13. Available from: <URL>.

14. Mani V, Park S, Kim JA, Lee SI, Lee K. Metabolic Perturbation and Synthetic Biology Strategies for Plant

Terpenoid Production—An Updated Overview. Plants. 2021;10(10):2179. Available from: <URL>.

15. Zhang Y, Song X, Lai Y, Mo Q, Yuan J. High-Yielding Terpene-Based Biofuel Production in Rhodobacter capsulatus. ACS Synth Biol. 2021;10(6):1545-1552. Available from: <URL>.

16. Pahima E, Hoz S, Ben-Tziona M, Majo DT. Computational design of biofuels from terpenes and terpenoids. Sustainable Energy Fuels. 2019;3:457-466. Available from: <URL>.

17. Alper Fitoz, Hasan Nazır, Mehtap Özgür (nee Yakut), Emel Emregül, Kaan C. Emregül, "An experimental and theoretical approach towards understanding the inhibitive behavior of a nitrile substituted coumarin compound as an effective acidic media inhibitor", Corrosion Science. 2018;133:451-464. Available from: <URL>.

18. Alper Fitoz, Zehra Yazan, "Experimental and theoretical approaches to interactions between DNA and purine metabolism products", International Journal of Biological Macromolecules. 2023;248:125961. Available from: <URL>.

19. A. Kalavathi, P. Saravana Kumar, K. Satheeshkumar, K.N. Vennila, S. Ciattini, L. Chelazzi, Kuppanagounder P. Elango, "Spectroscopic and TD-DFT studies on sequential fluorescent detection of Cu(II) and HS- ions in an aqueous solution", Inorganica Chimica Acta. 2023;550:121447. Available from: <URL>.

20. Maspero, A.; Vavassori, F.; Nardo, L.; Vesco, G.; Vitillo, J.G.; Penoni, A. Synthesis, Characterization, Fluorescence Properties, and DFT Modeling of Difluoroboron Biindolediketonates. Molecules. 2023;28:4688. Available from: <URL>.

21. McGarvey DJ, Croteau R. Terpenoid metabolism. Plant Cell. 1995;7(7):1015-1026. Available from: <URL>.

22. Vekiari SA, Protopapadakis EE, Papadopoulou P, Papanicolaou D, Panou C, Vamvakias M. Composition and seasonal variation of the essential oil from leaves and peel of a Cretan lemon variety. J Agric Food Chem. 2002;50(1):147-153. Available from: <URL>.

23. Al-Basheer W. Linear and nonlinear chiro-optical properties of carvone molecule mirror-image configurations. Proc SPIE. 2019;11026:110260Z. Available from: <URL>.

24. Sato H, Hashishin T, Kanazawa J, Miyamoto K, Uchiyama M. DFT Study of a Missing Piece in Brasilane-Type Structure Biosynthesis: An Unusual Skeletal Rearrangement. J Am Chem Soc. 2020;142(47):19830-19834. Available from: <URL>.

25. Sato H, Li BX, Takagi T, Wang C, Miyamoto K, Uchiyama M. DFT Study on the biosynthesis of verrucosane diterpenoids and mangicol sesterterpenoids: Involvement of secondary-carbocation-free reaction cascades. JACS Au. 2021;1(8):1231-1239. Available from: <URL>.

26. Zhu XK, Zheng YQ, Liu JB. A Computational Mechanistic Study of Cp*Co(III)-Catalyzed Three-Component C–H Bond Addition to Terpenes and Formaldehydes: Insights into the Origins of Regioselectivity. J Phys Chem A. 2021;125(23):5031-5039. Available from: <URL>.

27. Yankova R, Dimov M, Dobreva K, Stoyanova A. Electronic structure, reactivity, and Hirshfeld surface analysis of carvone. J Chem Res. 2019;43(9-10):319-29. Available from: <URL>.

28. Mekkaoui AA, El Ayouchia H, Anane H, Chahboun R, El Firdoussi L, El Houssame S. Viable route and DFT study for the synthesis of optically active limonaketone: A barely available natural feedstock in Cedrus atlantica. J Mol Struct. 2021;1235:130221. Available from: <URL>.

29. Becke AD. A new mixing of Hartree–Fock and local density-functional theories. J Chem Phys. 1993;98:1372-1377. Available from: <URL>.

30. Lee C, Yang W, Parr RG. Development of the Colle-Salvetti correlation-energy formula into a functional of the electron density. Phys Rev B. 1988;37:785-789. Available from: <URL>.

31. Raghavachari K, Binkley JS, Seeger R, Pople JA. Self-Consistent Molecular Orbital Methods. 20. Basis set for correlated wave-functions. J Chem Phys. 1980;72(1):650-654. Available from: <URL>.

32. McLean AD, Chandler GS. Contracted Gaussian-basis sets for molecular calculations. 1. 2nd row atoms, Z=11-18. J Chem Phys. 1980;72(9):5639-5648. Available from: <URL>.

33. Li X, Frisch MJ. Energy-represented DIIS within a hybrid geometry optimization method. J Chem Theory Comput. 2006;2(3):835-839. Available from: <URL>.

34. Kudin KN, Scuseria GE, Cancès E. A black-box self-consistent field convergence algorithm: One step closer. J Chem Phys. 2002;116(19):8255-8261. Available from: <URL>.

35. Frisch MJ, Trucks GW, Schlegel HB, Scuseria GE, Robb MA, Cheeseman JR, et al. Gaussian 09W, Revision D.01, Gaussian, Inc, Wallingford CT, 2013.

36. Dennington R, Keith TA, Millam JM. GaussView, Version 6. Semichem Inc., Shawnee Mission, KS, 2016.

37. Cossi M, Barone V, Cammi R, Tomasi J. Ab initio study of solvated molecules: A new implementation of the polarizable continuum model. Chem Phys Lett 1996;255:327-335. Available from: <URL>.

38. Tomasi J, Mennucci B, Cammi R. Quantum mechanical continuum solvation models. Chem Rev. 2005;105:2999-3093. Available from: <URL>.

39. McQuarrie DA. Statistical Thermodynamics. Harper & Row Publishers, 1973.

40. Hill TL. An Introduction to Statistical Thermodynamics. Addison-Wesley Publishing, 1962.

41. Herzberg, G. Molecular Spectra and Molecular Structure III (1st ed.). D. Van Nostrand Company, Inc., 1964.

42. Serdaroglu G, Durmaz S. DFT and statistical mechanics entropy calculations of diatomic and polyatomic molecules. Indian J Chem 2010; 49: 861-866. ISSN: 0376-4710

43. Koopmans T. Über die Zuordnung von Wellenfunktionen und Eigenwertenzu den Einzelnen Elektronen Eines Atoms. Physica 1934;1:104-113. Available from: <URL>.

44. Perdew JP, Parr RG, Levy M, Balduz JL, et al. Density-Functional Theory for Fractional Particle Number: Derivative Discontinuities of the Energy. Phys Rev Lett 1982;49(23):1691-1694. Available from: <URL>.

45. Janak JF. Proof that $\partial E/\partial n_i=\varepsilon_i$ in density-functional theory. Phys Rev B. 1978;18(12):7165-7168. Available from: <URL>.

46. Perdew JP, Levy M. Physical Content of the Exact Kohn-Sham Orbital Energies: Band Gaps and Derivative Discontinuities. Phys Rev Lett. 1983;51(20):1884-1887. Available from: <URL>.

47. Parr RG, Pearson RG. Absolute hardness: companion parameter to absolute electronegativity. J Am Chem Soc. 1983;105:7512-7516. Available from: <URL>.

48. Pearson RG. Absolute electronegativity and hardness correlated with molecular orbital theory. Proc Natl Acad Sci USA. 1986;83:8440-8441. Available from: <URL>.

49. Parr RG, Szentpaly LV, Liu S. Electrophilicity Index. J Am Chem Soc. 1999;121:1922-1924. Available from: <URL>.

50. Gazquez JL, Cedillo A, Vela A. Electrodonating and Electroaccepting Powers. J Phys Chem A. 2007;111(10):1966-1970. Available from: <URL>.

51. Gomez B, Likhanova NV, Domínguez-Aguilar MA, Martínez-Palou R, Vela A, Gazquez JL. Quantum Chemical Study of the Inhibitive Properties of 2-Pyridyl-Azoles. J Phys Chem B. 2006;110(18):8928-8934. Available from: <URL>.

52. NBO Version 3.1, E. D. Glendening, A. E. Reed, J. E. Carpenter, F. Weinhold.

53. J. P. Foster and F. Weinhold, "Natural hybrid orbitals", J. Am. Chem. Soc., 102 (1980):7211-7218.

54. Reed, A.E., Weinstock, R.B. and Weinhold, F. Natural Atomic Orbitals and Natural Population Analysis. Journal of Chemical Physics. 1985;83:735-746. Available from: <URL>.

55. A. E. Reed and F. Weinhold, "Natural localized molecular orbitals", J. Chem. Phys. 1985;83:1736-1740.

56. A. E. Reed, L. A. Curtiss and F. Weinhold, "Intermolecular interactions from a natural bond orbital, donor-acceptor viewpoint", Chem. Rev. 1988;88(6):899–926.

57. Mulliken RS. Chemical bonding. Annual Review of Physical Chemistry. 1978;29(1):1-31.

58. Daina A, Michielin O, Zoete V. iLOGP: A Simple, Robust, and Efficient Description of n-Octanol/Water Partition Coefficient for Drug Design Using the GB/SA Approach. J Chem Inf Model. 2014;54(12):3284–3301. Available from: <URL>.

59. Cheng T, Zhao Y, Li X, Lin F, Xu Y, Zhang X, Li Y, Wang R. Computation of Octanol−Water Partition Coefficients by Guiding an Additive Model with Knowledge. J Chem Inf Model. 2007;47(6):2140–2148. Available from: <URL>.

60. Wildman SA, Crippen GM. Prediction of Physicochemical Parameters by Atomic Contributions. J

Chem Inf Comput Sci. 1999;39:868-873. Available from: <URL>.

61. Lipinski CA, Lombardo F, Dominy BW, Feeney PJ. Experimental and computational approaches to estimate solubility and permeability in drug discovery and development settings. Adv Drug Deliv Rev. 2001;46:3–26. Available from: <URL>.

62. Silicos-it. (n.d.). Available from: <URL>.

63. Daina A, Michielin O, Zoete V. SwissADME: a free web tool to evaluate pharmacokinetics, druglikeness and medicinal chemistry friendliness of small molecules. Sci Rep. 2017;7:42717. Available from: <URL>.

64. Delaney JS. ESOL: Estimating Aqueous Solubility Directly from Molecular Structure. J Chem Inf Comput Sci. 2004;44:1000-1005. Available from: <URL>.

65. Ali J, Camilleri P, Brown MB, Hutt AJ, Kirton SB. In Silico Prediction of Aqueous Solubility Using Simple QSPR Models: The Importance of Phenol and Phenol-like Moieties. J Chem Inf Model. 2012;52:2950−2957. Available from: <URL>.

66. Ghose AK, Viswanadhan VN, Wendoloski JJ. A Knowledge-Based Approach in Designing Combinatorial or Medicinal Chemistry Libraries for Drug Discovery. 1. A Qualitative and Quantitative Characterization of Known Drug Databases. J Comb Chem. 1999;1:55-68. Available from: <URL>.

67. Veber DF, Johnson SR, Cheng H-Y, Smith BR, Ward KW, Kopple KD. Molecular Properties That Influence the Oral Bioavailability of Drug Candidates. J Med Chem. 2002; 45: 2615-2623. Available from: <URL>.

68. Egan WJ, Merz KM Jr, Baldwin JJ. Prediction of Drug Absorption Using Multivariate Statistics. J Med Chem. 2000; 43: 3867-3877. Available from: <URL>.

69. Muegge I, Heald SL, Brittelli D. Simple Selection Criteria for Drug-like Chemical Matter. J Med Chem. 2001;44(12):1841–1846. Available from: <URL>.

70. Martin YC. A Bioavailability Score. J Med Chem. 2005;48:3164-3170. Available from: <URL>.

71. ADMETlab 2.0.

72. Serin S. A comprehensive DFT study on organosilicon-derived fungicide flusilazole and its germanium analogue: A computational approach to Si/Ge bioisosterism. J Indian Chem Soc. 2023;100:100939. Available from: <URL>.

73. Serdaroğlu G, Ortiz JV. Ab Initio Calculations on some Antiepileptic Drugs such as Phenytoin, Phenbarbital, Ethosuximide and Carbamazepine. Struct Chem. 2017;28(4):957-964. Available from: <URL>.

74. Serdaroğlu G. DFT and Ab initio computational study on the reactivity sites of the GABA and its agonists, such as CACA, TACA, DABA, and muscimol: In the gas phase and dielectric media. Int J Quantum Chem. 2011;111(14):3938-3948. Available from: <URL>.

75. Serdaroğlu G. A DFT study of determination of the reactive sites of the acetylcholine and its agonists: In the gas phase and dielectric medium. Int J Quantum Chem. 2011;111(10):2464-2475. Available from: <URL>.

76. Serin S, Kaya G, Utku T. Insights into solvent effects on molecular properties, physicochemical parameters, and NLO behavior of brinzolamide, a bioactive sulfonamide: A computational study. J Indian Chem Soc. 2022;99:100738. Available from: <URL>.

77. Lin JH, Lu AY. Role of Pharmacokinetics and Metabolism in Drug Discovery and Development. Pharmacol Rev. 1997;49(4):403-449. Available from: <URL>.

78. Jackson E, Shoemaker R, Larian N, Cassis L. Adipose Tissue as a Site of Toxin Accumulation. Compr Physiol. 2017;7(4):1085–1135. Available from: <URL>.

79. Carpenter JF, Pikal MJ, Chang BS, Randolph TW. Rational design of stable lyophilized protein formulations: Theory and practice. Pharm Biotechnol. 1997;9:189-227. Available from: <URL>.

80. McGeer JC, Brix KV, Skeaff JM, DeForest DK, Brigham SI, Adams WJ, Green A. Inverse relationship between bioconcentration factor and exposure concentration for metals: implications for hazard assessment of metals in the aquatic environment. Environ Toxicol Chem. 2003;22(5):1017-1037. Available from: <URL>.

81. Nendza M, Müller M. Screening for low aquatic bioaccumulation. 1. Lipinski's 'Rule of 5' and molecular size. SAR QSAR Environ Res. 2010;21(5-6):495-512. Available from: <URL>.

82. Cuadros-Siguas CF, Herrera-Calderon O, Batiha GES, Almohmad, NH, Aljarba NH, Apesteguia-Infantes JA, ... & Pari-Olarte JB. Volatile Components, Antioxidant and Phytotoxic Activity of the Essential Oil of Piper acutifolium Ruiz & Pav. from Peru. Molecules. 2023;28(8):3348.

83. Rezende ECN, Carneiro FM, de Moraes JB, Wastowski IJ. Trends in science on glyphosate toxicity: a scientometric study. Environ Sci Pollut Res. 2021;28:56432–56448. Available from: <URL>.

84. Rivas-Garcia, T.; Espinosa-Calderón, A.; Hernández-Vázquez, B.; Schwentesius-Rindermann, R. Overview of Environmental and Health Effects Related to Glyphosate Usage. Sustainability. 2022;14:6868. Available from: <URL>.

85. Deeksha Rawat, Aarti Bains, Prince Chawla, Ravinder Kaushik, Rahul Yadav, Anil Kumar, Kandi Sridhar, Minaxi Sharma, Hazardous impacts of glyphosate on human and environment health: Occurrence and detection in food, Chemosphere. 2023;329:138676. Available from: <URL>.

86. Erdogan M, Serdaroglu G. New Hybrid (E)-4-((pyren-1-ylmethylene)amino)-N-(thiazol-2-yl)benzenesulfonamide as a Potential Drug Candidate: Spectroscopy, TD-DFT, NBO, FMO, and MEP Studies. Chemistry Select. 2021;6:9369–9381. Available from: <URL>.

87. Serdaroğlu G. Harmine derivatives: a comprehensive quantum chemical investigation of the structural, electronic (FMO, NBO, and MEP), and spectroscopic (FT-IR and UV–Vis) properties. Research on Chemical Intermediates. 2020;46(1):961-982.

88. Uludağ N, Serdaroğlu G. An efficient studies on C-2 cyanomethylation of the indole synthesis: The electronic and spectroscopic characterization (FT-IR, NMR, UV-Vis), antioxidant activity, and theoretical calculations. Journal of Molecular Structure. 2022;1247:131416.

89. Sigfridsson E, Ryde U. Comparison of methods for deriving atomic charges from the electrostatic potential and moments. Journal of Computational Chemistry. 1998;19(4):377-395. Available from: <URL>.

90. Serin S. DFT-based computations on some structurally related N-substituted piperazine. J Indian Chem Soc. 2022;99:100766. Available from: <URL>.

91. Hsissou R, Benhiba F, Echihi S, Benzidia B, Cherrouf S, Haldhar R, Alvi PA, Kaya S, Serdaroglu G, Zarrouk A. Performance of curing epoxy resin as potential anticorrosive coating for carbon steel in 3.5 NaCl medium: Combining experimental and computational approaches. Chem Phys Lett. 2021;783:139081. Available from: <URL>.